

Quantum phase transitions in spiral magnets without an inversion center

S V Demishev, V V Glushkov, S V Grigoriev, M I Gilmanov, I I Lobanova,
A N Samarin, A V Semeno, N E Sluchanko

DOI: 10.3367/UFNe.2016.02.037767

Contents

1. Introduction	559
2. Magnetic phase diagram of $Mn_{1-x}Fe_xSi$ solid solutions	560
3. Experimental verification of the theoretical model	560
4. Hall effect and nature of quantum criticality in $Mn_{1-x}Fe_xSi$	561
5. Conclusion	563
References	563

Abstract. It is shown that the $T-x$ magnetic phase diagram of $Mn_{1-x}Fe_xSi$ substitutional solid solutions exhibits two quantum critical points: $x^* \sim 0.11$, which corresponds to the disappearance of long-range spiral magnetic order, and $x_c \sim 0.24$, which marks the suppression of the phase with short-range magnetic order. It is established that the microscopic reason for the observed complicated quantum critical behavior is the evolution of the Fermi surface structure driven by an increase in iron concentration.

Keywords: spiral magnets, $Mn_{1-x}Fe_xSi$, quantum criticality, magnetic phase diagram, electron paramagnetic resonance, Hall effect, strongly correlated electron systems

S V Demishev Prokhorov General Physics Institute, Russian Academy of Sciences, ul. Vavilova 38, 119991 Moscow, Russian Federation; National Research University ‘Higher School of Economics’, ul. Myasnitskaya 20, 101000 Moscow, Russian Federation E-mail: demis@lt.gpi.ru

V V Glushkov, I I Lobanova, A V Semeno, N E Sluchanko Prokhorov General Physics Institute, Russian Academy of Sciences, ul. Vavilova 38, 119991 Moscow, Russian Federation; Moscow Institute of Physics and Technology (State University), Institutskii per. 9, 141700 Dolgoprudnyi, Moscow region, Russian Federation E-mail: glushkov@lt.gpi.ru, lobanova@lt.gpi.ru, semeno@lt.gpi.ru, nes@lt.gpi.ru

S V Grigoriev National Research Centre ‘Kurchatov Institute’, Konstantinov Petersburg Nuclear Physics Institute, Orlova roshcha, 188300 Gatchina, Leningrad region, Russian Federation E-mail: grigor@lns.pnpi.spb.ru

M I Gilmanov, A N Samarin Moscow Institute of Physics and Technology (State University), Institutskii per. 9, 141700 Dolgoprudnyi, Moscow region, Russian Federation E-mail: wlesavo@gmail.com, sasha@lt.gpi.ru

Received 3 March 2016

Uspekhi Fizicheskikh Nauk 186 (6) 628 – 632 (2016)

DOI: 10.3367/UFNr.2016.02.037767

Translated by A L Chekhov; edited by A Radzig

1. Introduction

Spiral magnets without an inversion center have recently started to attract much attention of researchers. One of the main reasons is the experimental implementation of special magnetic vortex structures — skyrmions [1, 2]. However, skyrmion issues do not limit the broad spectrum of physical phenomena which are inherent in this class of materials. Particularly, the study of quantum phase transitions is of great fundamental interest as well. These transitions can occur under a high pressure [3] or can be induced by changing the sample composition [4]. The present paper reports the investigation of quantum critical phenomena in $Mn_{1-x}Fe_xSi$ single-crystal solid solutions for $x < 0.3$. These materials are metals, in which the spiral magnetic structure originates due to the combination of ferromagnetic exchange interaction and the Dzyaloshinsky–Moriya interaction, which is allowed by the symmetry [4, 5]. The crystal structure of $Mn_{1-x}Fe_xSi$ is demonstrated in Fig. 1.

Quantum phase transitions are defined as those that occur at absolute zero temperature, $T = 0$, and the corresponding point on the control parameter axis is called the quantum critical point (QCP) [6]. For compounds based on manganese silicides, $MnSi$, theoretical models predict the existence of the

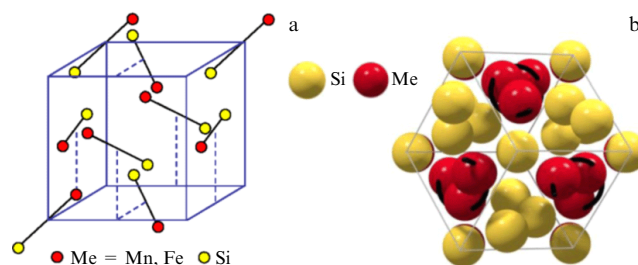


Figure 1. (a) Schematic of the structure of $Mn_{1-x}Fe_xSi$ substitutional solid solutions (structural type, B20). (b) View of the structure depicted in figure a, along the direction [111].

QCP, which separates phases with spiral long-range magnetic order (LRO) and short-range magnetic order (SRO) [7, 8]. The latter phase is often mentioned in the literature as the chiral spin liquid phase [7]. In the experiment, the QCP manifests itself in anomalous physical properties (for example, resistivity ρ or magnetic susceptibility χ) for $T > 0$ in the paramagnetic phase [6]. However, the situation is more complicated in the case of $\text{Mn}_{1-x}\text{Fe}_x\text{Si}$, because the QCP appears to be closed by the dome of the short-range magnetic order phase. This makes it nontrivial to observe phenomena indicating the quantum critical regime.

2. Magnetic phase diagram of $\text{Mn}_{1-x}\text{Fe}_x\text{Si}$ solid solutions

The T - x magnetic phase diagram of $\text{Mn}_{1-x}\text{Fe}_x\text{Si}$ solid solutions was defined from the correlation which was revealed in paper [9] between the qualitative change in small-angle neutron scattering (SANS) maps and the features in the $\chi(T)$ temperature dependence. We have found that the transition to the LRO-phase corresponds to the maximum of derivative $\partial\chi/\partial T$, and transition to the SRO-phase corresponds to the minimum of this derivative. Moreover, in order to define the point where the ferromagnetic correlations occur, the field dependences of magnetization in the Belov–Arrot coordinates can be analyzed [10]. The obtained T - x magnetic phase diagram is shown in Fig. 2a. It is evident that an increase in the iron concentration x lowers at first the temperature T_c of the transition into the phase with

a long-range magnetic order which is expected to be fully suppressed at $x^* \sim 0.11$ – 0.12 . By decreasing the temperature in the region of $x < x^*$, first the transition to the SRO-phase is induced, while for $x > x^*$ the only phase boundary corresponds to the transition between the paramagnetic (PM) phase and the SRO-phase. The temperature $T_s(x)$ of the transition to the phase with short-range magnetic order also decreases as the iron concentration increases, and its extrapolation to the value $T_s(x) = 0$ gives a new characteristic concentration $x_c \sim 0.24$. It is interesting that in the region of $x > x_c$ the temperature dependence of the magnetic susceptibility follows the power law: $\chi(T) \sim 1/T^\xi$ with the exponent $\xi \sim 0.5$ – 0.6 [10]. The observed anomalous dependence $\chi(T)$ indicates the appearance of the disorder-driven quantum critical regime [11]. In this case, the main state turns out to be the Griffiths phase [11, 12] consisting of isolated spin clusters which are formed in the sample volume due to the dispersion of exchange interaction J .

Thus, the experimental data indicate that the $\text{Mn}_{1-x}\text{Fe}_x\text{Si}$ compound exhibits two quantum critical points, x^* and x_c , which correspond to the suppression of long- and short-range magnetic orders, respectively. Obviously, the point x^* is hidden (Fig. 2a). Such an interpretation of the magnetic phase diagram is confirmed by the theoretical model proposed in paper [10]. In the framework of the approach presented, it is assumed that the intermediate phases with a short-range magnetic order appear when with a decrease in temperature the magnetic fluctuation radius $R(T)$ increases and reaches some critical value depending on the disorder degree in the system. A specific feature of this model is the assumption of the coexistence of classical fluctuations and quantum critical spin fluctuations with the radii $R_{cl} \sim 1/(T - T_c)^\beta$ and $R_{qc} \sim 1/T$, respectively [6, 10]. As this takes place, one needs only one free parameter, which defines the amplitude of quantum critical fluctuations, for describing the T - x phase diagram (Fig. 2b). Interestingly, the hidden quantum critical point x^* produces in this case two new lines in the magnetic phase diagram, indicated by dashed lines. One of these lines is $x = x^*$, which divides the region of coexistence of classical and quantum critical fluctuations ($x < x^*$) and the region where only quantum critical fluctuations take place ($x > x^*$). The second line is the crossover line $T_{eq}(x)$, which is defined by the condition $R_{cl}(T) = R_{qc}(T)$ (classical fluctuations are dominant in the left-hand region with respect to the crossover line).

3. Experimental verification of the theoretical model

Previous investigations gave evidence that magnetic scattering makes the main contribution to the transport properties of $\text{Mn}_{1-x}\text{Fe}_x\text{Si}$ [13], which means that the resistivity $\rho(T, x)$ will depend on the spin fluctuation behavior. For low temperatures, the temperature dependences of $\rho(T, x)$ for $\text{Mn}_{1-x}\text{Fe}_x\text{Si}$ can be described as $\rho(T, x) = \rho_0 + AT^\alpha$. The residual resistance ρ_0 can be defined in the experiment by extrapolating the given approximation to the zero temperature $T = 0$. Therefore, in order to detect the fine features of magnetic scattering, the temperature dependences of the resistivity were transformed into the form $\alpha(T, x) = \ln[(\rho - \rho_0)/A(T_s, x)]/\ln T$. This permits excluding changes in the parameter ρ_0 , which are not associated with the magnetic scattering and are caused, for example, by uncontrolled impurities. Figure 3 displays a map of $\alpha(T, x)$ obtained

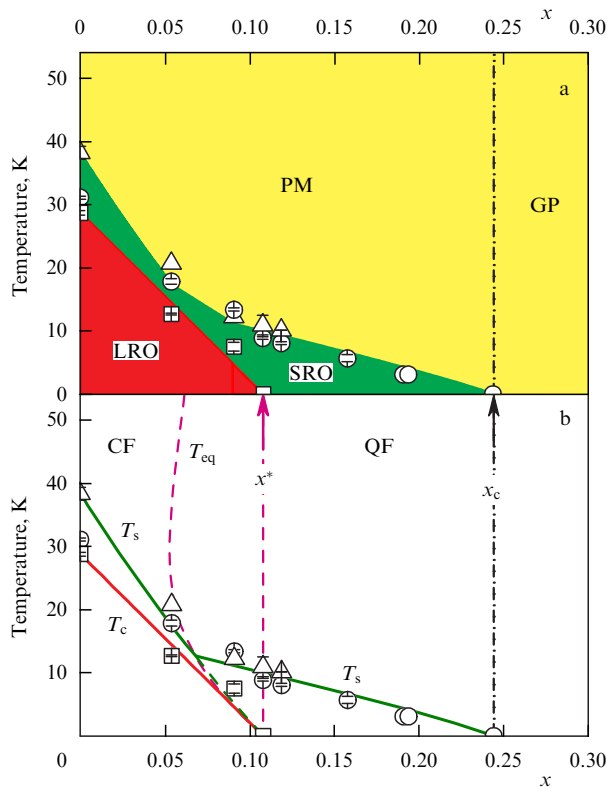


Figure 2. Magnetic phase diagram of $\text{Mn}_{1-x}\text{Fe}_x\text{Si}$: (a) experimental, and (b) theoretical results; PM—paramagnetic phase, and GP—Griffiths phase; CF and QF are, correspondingly, regions with dominant classical and quantum critical fluctuations. (Based on the data taken from Ref. [10].)

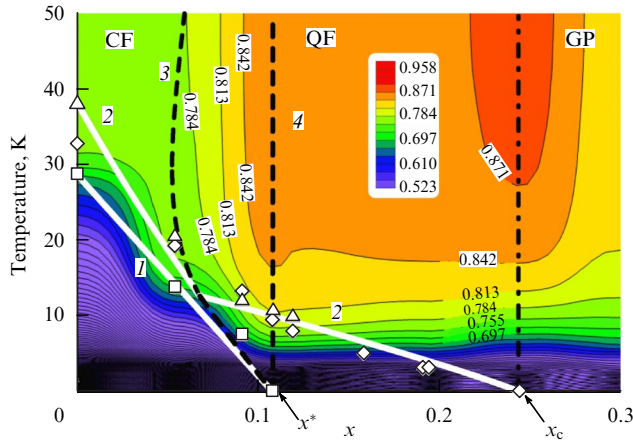


Figure 3. (Color online.) The $\alpha(T, x)$ map: line 1 — $T_c(x)$, 2 — $T_s(x)$, 3 — $T_{eq}(x)$, and 4 — $x = x_c$. The remaining notations are the same as in Fig. 2 (see details in the text).

in this way. It is interesting that the features of $\alpha(T, x)$ in the paramagnetic phase occur not only in the vicinity of the quantum critical point $x_c \sim 0.24$, but also appear to be connected with new lines in the magnetic phase diagram, which are associated with the existence of a hidden quantum critical point $x^* \sim 0.11$. Indeed, the exponent α increases exactly between the crossover line $T_{eq}(x)$ and the line $x = x^*$, i.e., in the parameter region where, according to Ref. [10], a change in the spin fluctuation regime in the paramagnetic phase should be observed. This allows concluding that the assumption of the existence of a hidden quantum critical point in the $\text{Mn}_{1-x}\text{Fe}_x\text{Si}$ system receives a support in experiment.

Another method for ‘visualization’ of quantum critical points in the $T-x$ magnetic phase diagram was proposed in paper [14], where the $\text{Mn}_{1-x}\text{Fe}_x\text{Si}$ system was investigated using the electron paramagnetic resonance (EPR) method. It was revealed that the EPR line shape corresponds to magnetic oscillations of localized magnetic moments of the manganese ions, and its width W is defined by the characteristic time and amplitude of spin fluctuations [14]. Temperature dependences $W(T)$ for samples with different iron concentrations are plotted in Fig. 4. It can be seen that the substitution of iron for manganese increases the EPR line width, and the temperature dependence $W(T)$ weakens in the vicinity of quantum critical points x^* and x_c . Such a peculiarity of spin relaxation was predicted in the EPR theory for strongly correlated metals, which was developed by Abrahams and Wölfle [15]. Using the temperature-dependent contribution to the line width revealed in Ref. [15], we can derive the expression $W(T) = W_1 T \arctan(T/T_x) + W_0$, where W_1 and W_0 are some constants, and T_x is the energy scale which sets the transition from the Fermi liquid regime ($T \ll T_x$) to the non-Fermi liquid regime ($T \gg T_x$) [14, 15]. Theoretical dependence $W(T)$ well describes the experimental data for samples with $x = 0.11 \sim x^*$ and $x = 0.24 \sim x_c$ with parameters $T_x \sim 11$ K (curve 1 in Fig. 4) and $T_x \sim 0$ K (curve 2 in Fig. 4), respectively. By comparing this result with the data shown in Fig. 2, it can be concluded that the characteristic temperature T_x for $\text{Mn}_{1-x}\text{Fe}_x\text{Si}$ turns out to be on the order of temperature corresponding to the transition to the SRO-phase. We also see that an anomalous spin relaxation takes place for finite temperatures in the $T-x$ magnetic phase

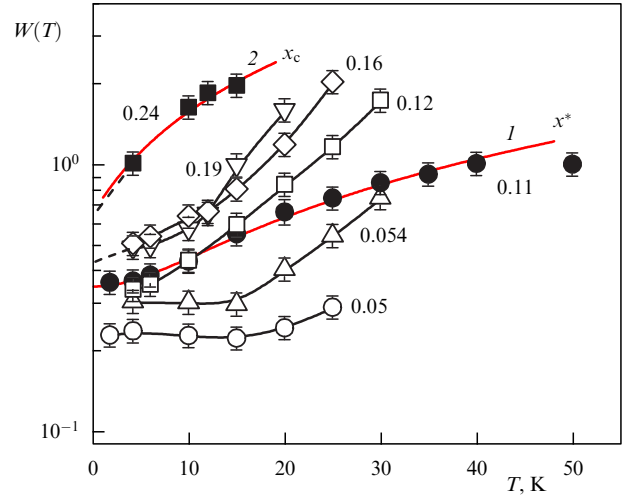


Figure 4. Temperature dependences of the EPR line width in the $\text{Mn}_{1-x}\text{Fe}_x\text{Si}$ system. Curves 1 and 2 are calculated results based on the Abrahams–Wölfle theory (see details in the text.). Numbers alongside the curves indicate the iron concentration. (Based on the results taken from paper [14].)

diagram along the lines $x = x^*$ and $x = x_c$, which is expected for quantum critical points.

4. Hall effect and nature of quantum criticality in $\text{Mn}_{1-x}\text{Fe}_x\text{Si}$

The experimental data obtained confirms the hypothesis of two successive quantum transitions which are responsible for the suppression of long-range and short-range magnetic orders in the $\text{Mn}_{1-x}\text{Fe}_x\text{Si}$ system. The decrease in $T_c(x)$ and disappearance of LRO can be explained by the decrease in the exchange energy $J(x)$ [10, 16], whereas the transition at $x = x_c$ can be explained by percolation effects, because for $x > x_c$ the magnetic subsystem of $\text{Mn}_{1-x}\text{Fe}_x\text{Si}$ splits into spin clusters and the concentration x_c can be related to the percolation threshold [10]. Such an interpretation corresponds to available experimental data, but it leaves two questions unanswered. First, comparing concentration dependences $T_c(x)$ and $J(x)$ allows one to make a conclusion that the transition temperature turns to zero before the exchange integral does [16]. Second, the manganese ion remains the most probable nearest neighbor of the manganese ion in the whole region $x < 0.3$. Therefore, we should understand the microscopic nature of quantum criticality, explain the divergence of $T_c(x)$ and $J(x)$, and define the mechanism responsible for percolation.

These questions were answered when investigating the Hall effect. For us, the most interesting results are the ones obtained from the normal Hall effect, which allow determining the concentration of charge carriers in the paramagnetic phase. However, an additional difficulty in the case of $\text{Mn}_{1-x}\text{Fe}_x\text{Si}$ is associated with the fact that the main contribution to the Hall resistivity ρ_H is due to the anomalous Hall effect. This led the authors of paper [17] to the pessimistic conclusion concerning the possibility to separate the normal component against the background of an anomalous component. We have overcome this ‘insolvable’ problem by analyzing the Hall resistivity in a weak magnetic field [18, 19]. The proposed method allowed us to demonstrate that the dependence of ρ_H on the magnetic field B and

temperature T in the $\text{Mn}_{1-x}\text{Fe}_x\text{Si}$ paramagnetic phase can be well described by the skew scattering model: $\rho_H = RB + S_1\rho(B, T)M(B, T)$, in which the normal Hall coefficient R and coefficient S_1 defining the magnitude of the anomalous contribution are functions of only iron concentration, and neither depend on the temperature or the magnetic field.

Obtained concentration dependences $R(x)$ and $S_1(x)$ are depicted in Fig. 5a. Both parameters change their sign when the iron content increases. It is interesting that the inversion of the S_1 sign at x_S occurs in the vicinity of the $T_{\text{eq}}(x)$ curve, which was predicted in paper [10] (Fig. 2b), and this parameter turns out to be sensitive to the change in the magnetic scattering regime. At the same time, the point x_R , where the normal Hall coefficient changes its sign, almost coincides with the hidden quantum critical point (see Figs 2, 5).

The experiment (see Fig. 5a) points to the fact that the substitution of iron for manganese induces hole doping. By using the standard two-band model [19], the experimental shape of the curve $R(x)$ (curve 1 in Fig. 5a) can be well described and the electron, $n(x)$, and hole, $p(x)$, concentrations can be found (Fig. 5b). Using the data obtained, the possibility appears to estimate the exchange interaction in the $\text{Mn}_{1-x}\text{Fe}_x\text{Si}$ compound. Although historically MnSi is assumed to be a typical itinerant magnet [20], a set of the latest experimental data on magnetic scattering [13] and EPR [14], as well as the local density approximation (LDA) calculations [21], clearly evidence the localization of spin density on the manganese ions. In this situation, one can apply the Ruderman–Kittel–Kasuya–Yosida (RKKY)

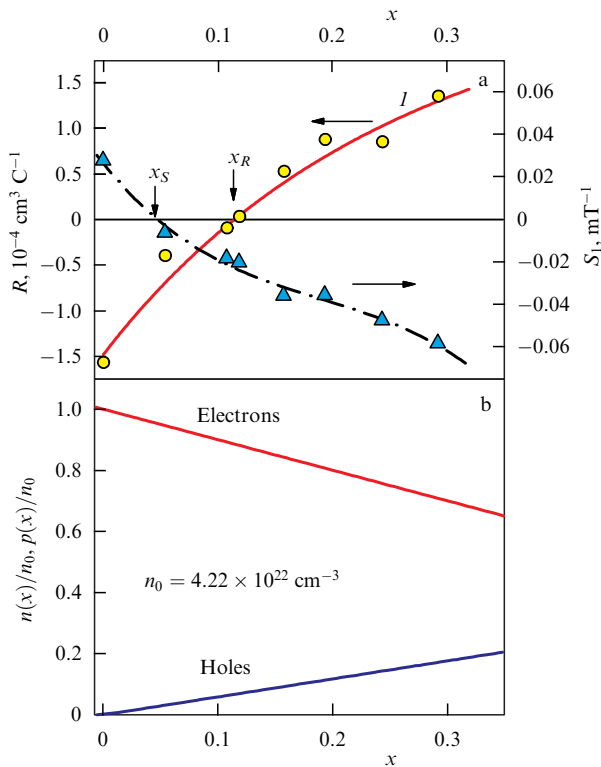


Figure 5. (a) Coefficients describing normal (R) and anomalous (S_1) Hall effects. Curve 1 — calculation based on the model with two charge carrier groups. (b) Change in the concentrations of electrons and holes in the $\text{Mn}_{1-x}\text{Fe}_x\text{Si}$ system, calculated from the model. (Based on the results taken from papers [18, 19]).

exchange model [22]. By assuming quadratic dispersion laws for electrons and holes, we can use the data from Fig. 5b and find the exchange integrals which describe interaction $J_1(x)$ between nearest neighbors (nn) and interaction $J_2(x)$ between next-nearest neighbors (nnn) [19].

The dependence of the RKKY interaction on the distance between manganese ions for pure MnSi is depicted in Fig. 6a. It can be seen that the nn-exchange is ferromagnetic, $J_1 > 0$, and the nnn-exchange is antiferromagnetic, $J_2 < 0$, which means that during the analysis of magnetic states in $\text{Mn}_{1-x}\text{Fe}_x\text{Si}$ we need to take into account the frustration effects. If both electrons and holes are present, the RKKY exchange depends on the ratio m_e/m_h between the effective masses of electrons and holes [19, 22], which can be determined from the condition of fitting the experimental curve $J(x)$ [16] with the theoretical dependence $J_1(x)$. The best match between the theory and the experiment was achieved at $m_e/m_h = 0.325$ (Fig. 6b).

After the ratio m_e/m_h is fixed, the nnn-exchange $J_2(x)$ can be found without using any additional parameters. We can see from Fig. 6 that $J_2(x) < 0$ over the whole range of $x < 0.3$, while the nn-exchange changes its sign at $x_J \sim 0.17$. Moreover, the following conditions are fulfilled in the vicinity of the hidden QCP x^* : $J_1 > 0$, $J_2 < 0$, and $|J_1| \sim |J_2|$. These conditions correspond to the strong frustration regime, which is responsible for the suppression of the long-range magnetic order. As a result, $T_c(x)$ turns to zero faster than $J(x)$, which one can observe in experiment [16]. In the region of compositions $x \sim x_c$, both exchange interactions, nn and nnn, are antiferromagnetic and frustration becomes significant, while the relationship $|J_1| \sim |J_2|$ holds true again (Fig. 6b). In this situation, it is reasonable to assume that the frustration effects in the vicinity of the second QCP, x_c ,

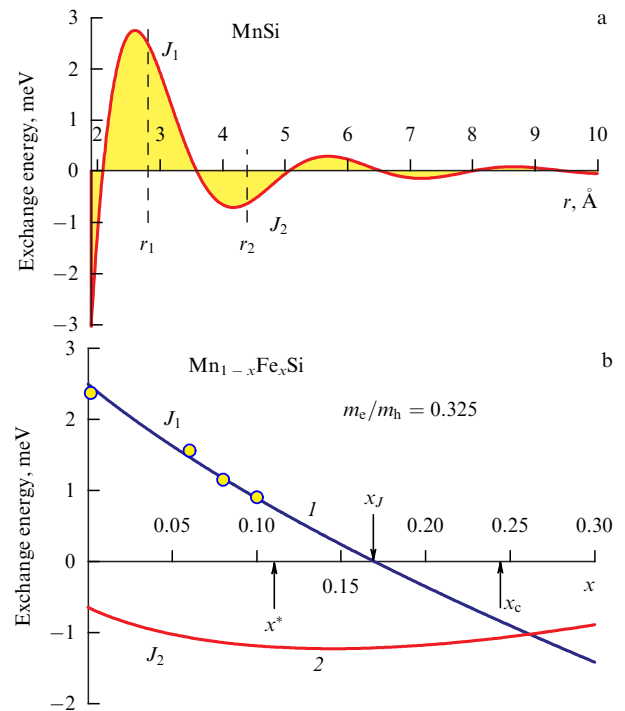


Figure 6. (a) RKKY function for MnSi; r_1 is the distance between nearest neighbors (nn), and r_2 is the distance to the next-nearest neighbors (nnn). (b) Changes of exchange energies J_1 (nn) and J_2 (nnn). Curves 1, 2 are the results of theoretical calculations; circles show the experimental data [16]. (Based on the results taken from paper [19]).

would facilitate the system to split into spin clusters forming the Griffiths phase.

It is interesting to note that modeling of frustration effects in MnSi in the absence of the Dzyaloshinsky–Moriya (DM) interaction gives evidence [23] that the frustration leads to the formation of magnetic spirals oriented along the direction [110], whereas the DM interaction orients the magnetic spirals in the zero magnetic field along the directions [111] (see Refs [5, 16]). Therefore, it should be expected that not only substitution disorder effects, but also interplay between frustration and DM interaction will lead to the suppression of long-range magnetic order and the formation of phases with short-range magnetic order in according to the observed $T-x$ magnetic phase diagram (see Fig. 2).

5. Conclusion

Summing up, we have shown that the quantum criticality in $\text{Mn}_{1-x}\text{Fe}_x\text{Si}$ is controlled by the changes in electron and hole concentrations, which influence the exchange energies, frustration, and substitution disorder effects through the RKKY interaction. Based on results of the present study, one can predict the character and evolution features of the Fermi surface structure for different solid solution compositions, as well as the replacement of the ferromagnetic type of exchange interaction between nearest neighbors by the antiferromagnetic one. Verification of these assumptions is a challenging task and can be performed in future investigations of the $\text{Mn}_{1-x}\text{Fe}_x\text{Si}$ system by methods of neutron diffractometry and angle-resolved photoemission spectroscopy (ARPES).

Acknowledgments

This study was supported by the RFBR grant No. 13-02-00160 and the RAS programs ‘Electron spin resonance, spin-dependent electron effects, and spin technologies’ and ‘Electron correlations in systems with strong interaction’.

References

- Mühlbauer S et al. *Science* **323** 915 (2009)
- Lobanova I I et al. *Sci. Rep.* **6** 22101 (2016)
- Pfleiderer C et al. *Phys. Rev. B* **55** 8330 (1997)
- Bauer A et al. *Phys. Rev. B* **82** 064404 (2010)
- Grigoriev S V et al. *Phys. Rev. B* **81** 012408 (2010)
- Sachdev S *Quantum Phase Transitions* (Cambridge: Cambridge Univ. Press, 2011)
- Tewari S, Belitz D, Kirkpatrick T R *Phys. Rev. Lett.* **96** 047207 (2006)
- Krüger F, Karahasanovic U, Green A G *Phys. Rev. Lett.* **108** 067003 (2012)
- Grigoriev S V et al. *Phys. Rev. B* **83** 224411 (2011)
- Demishev S V et al. *JETP Lett.* **98** 829 (2013); *Pis'ma Zh. Eksp. Teor. Fiz.* **98** 933 (2013)
- Bray A J *Phys. Rev. Lett.* **59** 586 (1987)
- Griffiths R B *Phys. Rev. Lett.* **23** 17 (1969)
- Demishev S V et al. *Phys. Rev. B* **85** 045131 (2012)
- Demishev S V et al. *JETP Lett.* **100** 28 (2014); *Pis'ma Zh. Eksp. Teor. Fiz.* **100** 30 (2014)
- Abrahams E, Wölfle P *Phys. Rev. B* **78** 104423 (2008)
- Grigoriev S V et al. *Phys. Rev. B* **79** 144417 (2009)
- Franz C et al. *Phys. Rev. Lett.* **112** 186601 (2014)
- Glushkov V V et al. *JETP Lett.* **101** 459 (2015); *Pis'ma Zh. Eksp. Teor. Fiz.* **101** 512 (2015)
- Glushkov V V et al. *Phys. Rev. Lett.* **115** 256601 (2015)
- Moriya T *Spin Fluctuations in Itinerant Electron Magnetism* (Berlin: Springer-Verlag, 1985); Translated into Russian: *Spinovye Fluktuatsii v Magnetikakh s Kollektivirovannymi Elektronami* (Moscow: Mir, 1988)
- Corti M et al. *Phys. Rev. B* **75** 115111 (2007)
- Vonsovskii S V *Magnetism* (New York: J. Wiley, 1974); Translated from Russian: *Magnetizm* (Moscow: Nauka, 1971)
- Hopkinson J M, Kee H-Y *Phys. Rev. B* **75** 064430 (2007)